Brain and muscle activity during fatiguing maximum-speed knee movement

Title: Brain and muscle activity during fatiguing maximum-speed knee movement

Running head: EEG and EMG in maximum-speed knee movement

José Pedro Correia[1,2], Christophe Domingos[3,4], Erik Witvrouw[5], Pedro Luís[6], Agostinho Rosa[6], João R. Vaz[2,7], Sandro R. Freitas[1]

[1]Laboratório de Função Neuromuscular, Faculdade de Motricidade Humana, Universidade de Lisboa, Cruz Quebrada, Portugal

[2]CIPER, Faculdade de Motricidade Humana, Universidade de Lisboa, Cruz Quebrada, Portugal

[3]Institute of Psychology, Department of Clinical Psychology, Jagiellonian University, Krakow, Poland

[4]CIEQV, Escola Superior de Desporto de Rio Maior, Instituto Politécnico de Santarém, Av. Dr. Mário Soares nº 110, 2040-413 Rio Maior, Portugal

[5]Department of Rehabilitation Sciences, Ghent University Faculty of Medicine and Health Sciences, Ghent, Belgium

[6]LaSEEB, Instituto Superior Técnico, Universidade de Lisboa, Lisboa, Portugal

[7]Egas Moniz Center for Interdisciplinary Research, Egas Moniz School of Health & Science, Monte da Caparica, Portugal

Author ORCiDs:

José Pedro Correia: 0000-0001-5331-8547
Christophe Domingos: 0000-0001-5855-1372
Erik Witvrouw: 0000-0002-1919-877X
Agostinho Rosa: 0000-0001-5165-3114
João R. Vaz: 0000-0001-9691-5456
Sandro R. Freitas: 0000-0002-9760-5350

Corresponding author:
José Pedro Correia
jpcorreia.ft@gmail.com

Acknowledgements: JPC is funded by a grant from Fundação para a Ciência e Tecnologia (SFRH/BD/143927/2019). This work is part of the HamStrong project which is supported by the Fundação para a Ciência e Tecnologia (grant: PTDC/SAU-DES/31497/2017); CD was supported by funding from Fundação para a Ciência e Tecnologia (grant: UIDP/04748/2020).

New & Noteworthy

The loss of knee movement rate with acute fatigue induced by high-speed movement is associated with both central and peripheral electrophysiological changes, such as a

decrease in EEG power, increased agonist-antagonist co-contraction, and impaired brain-muscle coupling. These findings had not previously been reported for the knee joint, which shows functional and physiological differences compared to the existing findings for smaller upper limb joints.

Abstract

While the underlying mechanisms behind upper limb (e.g., finger) motor slowing during movements performed at the maximum voluntary rate have been explored, the same cannot be said for the lower limb. This is especially relevant considering the lower limb's larger joints and different functional patterns. Despite the similar motor control base, previously found differences in movement patterns and segment inertia may lead to distinct central and peripheral manifestations of fatigue in larger joint movement. Therefore, we aimed to explore these manifestations in a fatiguing knee maximum movement rate task by measuring brain and muscle activity, as well as brain-muscle coupling using corticomuscular coherence, during this task. A significant decrease in knee movement rate up to half the task duration was observed. After an early peak, brain activity showed a generalized decrease during the first half of the task, followed by a plateau, while knee flexor muscle activity showed a continuous decline. A similar decline was also seen in corticomuscular coherence, but for both flexor and extensor muscles. The electrophysiological manifestations associated with knee motor slowing therefore showed some common and some distinct aspects compared to smaller joint tasks. Both central and peripheral manifestations of fatigue were observed; the changes seen in both EEG and EMG variables suggest that multiple mechanisms were involved in exercise regulation and fatigue development.

Keywords: movement rate, electroencephalography, electromyography, motor control, fatigue

Introduction

Repetitive unloaded movement at maximum voluntary rate has been shown to lead to decreases in movement rate; this phenomenon has been referred to as motor slowing (1–3). This performance loss is proposed to have a predominantly central origin (1, 2, 4). The involved mechanisms may include fatigue of intracortical inhibitory circuits, leading to less fluid (and thus slower) movement patterns (1, 3, 4). It has also been proposed that fatigue of the central motor command to switch between movement directions drives this decrease, manifested as a loss of a clear agonist/antagonist electromyographic (EMG) activity pattern (2). On a different perspective, Zanette et al. (5) found a significant decrease in the size of the motor representation area and decreased cortical excitability mediated by intracortical presynaptic modulation after a thumb adduction 1-min maximum voluntary rate task. Thus, uncertainties remain regarding the mechanisms of motor slowing in healthy individuals.

To the best of our knowledge, the patterns of brain and muscle activity associated with knee motor slowing have not been previously explored. While it is true that various motor control mechanisms have been shown to be similar across body regions (6–8), there are also factors that differentiate upper and lower limb motor control both at central and peripheral levels. Knee unilateral movements show less sensorimotor lateralization than finger and elbow movements on functional magnetic resonance imaging (fMRI) as well as differences to other lower limb joints (9, 10); lower limb joints have also shown a greater somatotopic sensorimotor and cerebellar overlap as well as different activation patterns compared to upper limb joints (11). As for peripheral differences, segment inertia has been shown to affect EMG activity patterns in fast/ballistic movements (6, 12, 13). The increased inertia of the leg compared to the fingers or wrist may lead to different EMG activity patterns. Additionally, the typical functional patterns of the upper (low load, asymmetrical, and fine motor skills) and lower (high load, symmetrical, and directed for balance and stability) extremities are distinct (14). Finally, changes in motoneuron excitability induced by fatigue have been shown to differ between the upper and lower limb (15, 16). Therefore, the physiology behind knee motor slowing may show important differences to the existing upper limb findings.

Additionally, this study can contribute to the debate on maximal exercise regulation mechanisms, considering the controversy on the degree of central and peripheral contributions, and respond to the need to determine the degree of cortical involvement in rhythmic movements.

In a previous preliminary study, we found significant knee motor slowing using the same task as in this study (17). In order to further substantiate those findings and to shed light on the associated physiological mechanisms, the main objective of this study is to determine what measures of brain and muscle activity are associated with the loss of knee movement rate with repetitive movement. As a secondary objective, considering the highly dynamic nature of the used task and the natural motor control variability, we aimed to evaluate the between-session group behavior and the test-retest reliability of these parameters.

Methods

Sampling and study criteria

A convenience sample was recruited from the local institution. Males between 18 to 39 years were included. Exclusion criteria were 1) a history of knee, hip, or central nervous system surgery; 2) a history of hip or knee structural musculoskeletal injury; 3) any contraindication to ventral decubitus; 4) any condition which prevented participants from performing the requested movement; 5) regular (>2 times/week) training of any sporting discipline. Males were chosen for this study since they show greater movement rates and performance decrement in maximal intermittent tasks such as repeated sprinting (18, 19). This greater decrement makes significant changes both in performance and in the associated physiological variables more likely to be detected, providing greater insight into regulatory mechanisms. The age limit was placed since that is the threshold after which the maximum motor speed starts to decrease (20).

The study was approved by the local institutional review board (approval number: 8/2021) and all participants provided written informed consent. Sample size calculation was performed using G*Power 3.1.9.4 (Heinrich-Heine-Universität Düsseldorf, Düsseldorf, Germany). Considering changes in movement rate during the task, a sample size of 20 individuals was required to achieve a power of 0.95 with a partial eta squared effect size (η_p^2)=0.15 over eight repeated measurements.

Experimental protocol

Participants undertook two experimental sessions separated by at least a week. Upon arrival, anthropometric data (age, height, body mass) were collected. Participants then completed a 5-min warm-up on a stationary bicycle at a comfortable rate (≈70 rpm) without added resistance. Subsequently, participants were placed in the prone position on a table and asked to perform unloaded bilateral alternating knee flexion/extension movements at their maximum voluntary rate over eight blocks of 10 s with 5 s of rest between blocks (Figure 1). Movements were performed in the 45-90° range (Figure 1); before starting, participants were familiarized with this range of motion as long as needed through the use of soft bumpers. Afterwards, these bumpers were removed, and participants performed 2-3 s of knee flexion/extension movements at the maximum voluntary rate to confirm they had correctly familiarized themselves with the desired range of motion. The accuracy of the range of motion using this familiarization was confirmed previously (17).

We chose a short movement arc to increase the direction change challenge, since it has been reported that increased cortical activity is needed for the change between flexor and extensor movement (21). The prone position was chosen since we aimed to design a task in which the anti-gravity work was performed by the knee flexors and to remove visual feedback, as it has been shown to affect the control of high-speed movements (14). Participants were instructed to maintain their movement rate as high as possible throughout the entire task through verbal encouragement and were instructed to make any corrections to the range of motion if needed. Brain activity, muscle activity, and movement rate were monitored during this task using electroencephalography, electromyography, and accelerometry, respectively. The experimental setup is depicted in figure 1.

Electroencephalography

A 24-channel EEG device (Vertex SC823, Meditron Eletromedicina Ltda, São Paulo, Brazil) was used according to the international 10–20 system with online referencing to two electrodes placed at the mastoid processes; the sampling frequency was 250 Hz and electrode configuration was as shown in figure 1. Before starting data collection, a circuit impedance ≤10 kΩ was ensured in all electrodes, and an analog band-pass filter (0.1-70 Hz) was applied by the amplifier.

Electromyography and accelerometry

Five wireless electrodes (Trigno, Delsys, Natick, MA) were placed on the right vastus lateralis (VL), rectus femoris (RF), vastus medialis (VM), biceps femoris (BF), and semitendinosus (ST) according to SENIAM recommendations (22) and secured with

adhesive tape. Prior to electrode placement, the skin was shaved and cleaned with alcohol to decrease skin impedance. EMG data were collected at a sampling frequency of 1926 Hz. The EMG system applied a bandpass filter of 10-850 Hz. Two additional electrodes were placed on the lateral malleoli to collect accelerometry data at a sampling frequency of 148 Hz.

As in previous studies of bilateral lower limb movement rate, we did not differentiate individuals according to dominance (23, 24). EMG data were assessed on the right limb. This approach was used since the main focus was on the central motor control aspects of fast movements; the left hemisphere (which is primarily responsible for right limb movement) has been shown to have a degree of specialization in controlling fast repetitive movement (25, 26), and there is a different association with dominance in the structure of the left and right hemispheres (27).

Data processing

Data were processed using Matlab scripts (MathWorks Inc., Natick, MA) (supplementary file S1, https://doi.org/10.5281/zenodo.7704280). To analyze the EEG and EMG signals, we discarded the first and last seconds of each movement block of EEG and EMG signals to achieve better signal stability, resulting in 8-s periods for each block. For the movement rate calculation, the entire 10-s period was used since it is not affected by signal stability. Movement rate was determined using the number of accelerometer peaks during each block; the presented values correspond to the movement rate of each limb.

EEG data were high-pass filtered at 1 Hz, notch filtered at 50 Hz to remove line noise, and low-pass filtered at 50 Hz using fourth-order, zero-lag Butterworth filters. Independent component analysis was performed using EEGLAB (28) to remove muscle, eye, line noise, mechanical, and other artifacts from the filtered EEG signal using visual inspection to determine the components to be removed. Artifacts were identified based on their waveform and biological plausibility. If these artifacts could not be removed in an isolated manner using independent component analysis, artifact subspace reconstruction was used to minimize signal loss. The EEG power was calculated for the theta (4-7.9 Hz), alpha (8-14.9 Hz), beta (15-30.9 Hz), and gamma (31-50 Hz) bands for each 8-s period of the task. We chose to analyze the EEG data up to 50 Hz since there is a negligible amount of signal content above this frequency in healthy individuals (29). We calculated two EEG power measures: each band's relative power as a percentage of the total signal power and the normalized power referenced to the first block. These parameters were calculated to account for the inter-individual variability and allow for more accurate comparisons. All EEG measures were calculated for four electrodes placed over areas associated with cortical motor planning and execution and which have been shown to have movement rate-associated activity: F3, F4, C3, and C4 (Figure 1).

EMG data were high-pass filtered at 20 Hz, notch filtered at 50 Hz to remove line noise, and low-pass filtered at 450 Hz using fourth-order, zero-lag Butterworth filters. The signal was then full-wave rectified and the root mean square (RMS) of the amplitude was calculated using 250 ms windows with a 125 ms overlap. The three 250-ms windows with the highest values were selected from each block, averaged, and normalized to the value from the first block. This normalization of EMG amplitude to that of a similar action being investigated has

been recommended for high-velocity muscle actions (30). Two EMG co-contraction indices were calculated as a measure of agonist-antagonist coordination; one between the VL and BF (CCI_{lat}) and another between the VM and ST (CCI_{med}). Both indices were calculated as the percentage of overlap between the RMS areas of the corresponding muscles for each block (31).

Corticomuscular coherence (CMC)

To analyze the time-frequency functional coupling of EEG and EMG signals, wavelet coherence was calculated as described by Yoshida et al.(23) using a publicly available MATLAB package (Wavelet Toolbox). Morlet wavelet coherence has previously been used in rhythmic tasks as it is a good choice in terms of time and frequency resolution in the analysis of nonstationary signals (23, 32). For the coherence analysis, EMG signals were high-pass filtered at 3 Hz (instead of 20 Hz) and downsampled to 250 Hz to match the EEG sampling rate. Wavelet coherence was determined in the 1-50 Hz range; the threshold for coherence significance (CT) was calculated using the following equation (23):

$$CT = 1 - \left[\frac{1}{N}\left(1 - \frac{\alpha}{100}\right)\right]^{\frac{1}{L-1}}$$

where *N* is the number of frequency bins and α is the confidence level (95% in our study). Considering the cyclic nature of our task, we defined L as the number of cycles completed by each participant, as done in a previous study using a task of this type (23). CMC was calculated between the signals of the C3 electrode and each muscle's EMG signal. Two coherence outcomes were used; first, the total area of coherence above the CT was calculated across the 1-50 Hz spectrum for each block. Second, time-frequency maps of the observed coherence were constructed to provide a qualitative CMC analysis.

Statistical analysis

Data normality was tested using the Shapiro-Wilk test. A two-way repeated measures ANOVA (2 sessions $\times$ 8 blocks) was used to test changes in movement rate, EEG power, EMG RMS, and significant CMC across the eight blocks and between the two sessions. Post-hoc testing with Bonferroni adjustment for multiple comparisons was made to determine significant differences between individual blocks (a total of 28 comparisons). Statistical analyses were performed using SPSS software (v25, IBM Corp., Armonk, NY). P-values <0.05 were considered significant. η_p^2 values were used as a measure of effect size and classified as small (0.01-0.06), medium (0.06-0.14), and large (>0.14) (33). The test-retest intraclass correlation coefficients (ICC) were calculated using a two-way mixed model and an absolute agreement definition (34). In cases where the assumptions for the use of parametric ICCs were violated (i.e., normality and homogeneity of variances (35)), a nonparametric concordance coefficient was calculated using the "nopaco" R package version 1.0.5 (36). Considering the number of variables in the electrophysiological analyses (EEG, EMG, and CMC), and in order to decrease the number of analyses, we determined the test-retest reliability of the percentage of change (block 1-block 8) and of the linear slope of the change over the eight blocks. These coefficients were classified as poor (<0.5),

moderate (0.5-0.75), good (0.76-0.9), and excellent (>0.9)(34). In addition to the ICCs, the test-retest standard error of measurement was also calculated as an index of reliability and calculated from the mean error term of the corresponding ANOVA, as it has the advantage of being independent of the ICC (37). Statistical analyses were performed using SPSS version 25 (IBM Corp., Armonk, NY) and R Studio version 1.2.5042 (Posit Software, Boston, MA).

Results

Nineteen participants (age: 25.9±6.4 years; height: 1.77±0.08 m; weight: 74.7±11.2 kg) were included in the study. The average gap between sessions was 9.1±3.4 days. We did not enroll the initially planned 20 participants since the intended power was already exceeded with this sample size.

Movement rate

There was a significant effect of the block factor, showing a decrease in movement rate ($p < 0.001$, $\eta_p^2=0.786$, power >0.99) but no significant differences between sessions ($p=0.079$, Figure 2). In both sessions, 93-96% of the decrease in movement rate occurred in the first four blocks. Post-hoc testing revealed significant differences between the first and second to fourth blocks and between the first three and last five blocks (Figure 2). There was no significant block × session interaction ($p=0.788$). The ICCs for the movement rate ranged from 0.74 to 0.92 (good to excellent) across movement blocks (Table 1).

Table 1. Movement rate test-retest ICC and SEM

Block	Test-retest ICC (95% CI)	Test-retest SEM (Hz)
1	0.852 (0.559 - 0.95)	0.20
2	0.805 (0.385 - 0.934)	0.16
3	0.891 (0.675 - 0.963)	0.15
4	0.740 (0.291 - 0.908)	0.23
5	0.888 (0.670 - 0.962)	0.14
6	0.915 (0.760 - 0.970)	0.14
7	0.912 (0.754 - 0.969)	0.13
8	0.858 (0.607 - 0.950)	0.16

ICC, intraclass correlation coefficient; CI, confidence interval; SEM, standard error of measurement

Electroencephalography

In the relative band power analysis, there was no significant effect of the block factor in any electrode (F4: p=0.340 to 0.573; F3: p=0.144 to 0.450; C4: p=0.242 to 0.660; C3: p=0.297 to 0.925), as well as no differences between sessions (F4: p=0.235 to 0.953; F3: p=0.382 to 0.919; C4: p=0.370 to 0.979; C3: p=0.078 to 0.563). The relative EEG power nonparametric concordance coefficients ranged from 0.62 to 0.77 (moderate to good) for the percentage of change from the first to the last block and from 0.65 to 0.82 (moderate to good) for the slope of the changes over the eight blocks (Table 2).

Table 2. Relative EEG power test-retest ICC and SEM

EEG channel	Frequency band	Parameter	Test-retest ICC (95% CI)	Test-retest SEM
F4	Theta	Pre-post	0.768 (0.626 - 1)	144.3%
		Slope	0.658 (0.547 - 1)	0.037
	Alpha	Pre-post	0.708 (0.597 - 1)	48.2%
		Slope	0.667 (0.573 - 1)	0.011
	Beta	Pre-post	0.623 (0.532 - 1)	43.4%
		Slope	0.756 (0.642 - 1)	0.016
	Gamma	Pre-post	0.689 (0.568 - 1)	82.2%
		Slope	0.652 (0.562 - 1)	0.008
F3	Theta	Pre-post	0.795 (0.674 - 1)	81.1%
		Slope	0.824 (0.716 - 1)	0.020
	Alpha	Pre-post	0.616 (0.515 - 1)	51.8%
		Slope	0.684 (0.579 - 1)	0.010
	Beta	Pre-post	0.669 (0.562 - 1)	46.0%

		Slope	0.740 (0.641 - 1)	0.010
	Gamma	Pre-post	0.722 (0.604 - 1)	88.3%
		Slope	0.694 (0.591 - 1)	0.010
C4	Theta	Pre-post	0.746 (0.631 - 1)	65.9%
		Slope	0.732 (0.616 - 1)	0.025
	Alpha	Pre-post	0.666 (0.554 - 1)	29.7%
		Slope	0.659 (0.582 - 1)	0.009
	Beta	Pre-post	0.680 (0.569 - 1)	44.9%
		Slope	0.738 (0.615 - 1)	0.013
	Gamma	Pre-post	0.683 (0.574 - 1)	127.7%
		Slope	0.675 (0.573 - 1)	0.015
C3	Theta	Pre-post	0.762 (0.648 - 1)	73.5%
		Slope	0.698 (0.576 - 1)	0.029
	Alpha	Pre-post	0.720 (0.601 - 1)	39.6%
		Slope	0.653 (0.571 - 1)	0.010
	Beta	Pre-post	0.744 (0.623 - 1)	81.7%
		Slope	0.762 (0.642 - 1)	0.014
	Gamma	Pre-post	0.723 (0.598 - 1)	155.1%
		Slope	0.678 (0.555 - 1)	0.009

ICC, intraclass correlation coefficient; CI, confidence interval; SEM, standard error of measurement

In the normalized EEG power analysis, a significant effect of the block factor in all frequency bands at the F4 (theta: $p=0.02$, $\eta_p^2=0.223$, power=0.78; alpha: $p=0.011$, $\eta_p^2=0.228$,

power=0.82; beta: p=0.002, η_p^2=0.286, power=0.93; gamma: p=0.013, η_p^2=0.223, power=0.81) and F3 electrodes (theta: p=0.02, η_p^2=0.247, power=0.77; alpha: p<0.001, η_p^2=0.311, power=0.96; beta: p=0.005, η_p^2=0.270, power=0.88; gamma: p=0.015, η_p^2=0.206, power=0.80) was observed. In the central electrodes, a significant effect of the block factor was only seen in the C3 electrode for the alpha (p=0.010, η_p^2=0.203, power=0.86) and beta (p=0.001, η_p^2=0.238, power=0.96) bands. The results of post-hoc testing regarding significant differences between individual blocks can be seen in figure 3. In general, these differences tended to show lower EEG power in the later blocks compared to the peak EEG power at the second or third block.

There were no significant differences in normalized EEG power between sessions in any electrode (F4: p=0.215 to 0.878; F3: p=0.363 to 0.553; C4: p=0.197 to 0.858; C3: p=0.287 to 0.289). The normalized EEG power nonparametric concordance coefficients ranged from 0.64 to 0.88 (moderate to good) for the percentage of change from the first to the last block and from 0.62 to 0.80 (moderate to good) for the slope of the changes over the eight blocks (Table 3).

Table 3. Normalized EEG power test-retest ICC and SEM

EEG channel	Frequency band	Parameter	Test-retest ICC (95% CI)	Test-retest SEM
F4	Theta	Pre-post	0.642 (0.523 - 1)	60.3%
		Slope	0.712 (0.608 - 1)	0.126
	Alpha	Pre-post	0.724 (0.596 - 1)	49.8%
		Slope	0.738 (0.628 - 1)	0.083
	Beta	Pre-post	0.688 (0.594 - 1)	41.5%
		Slope	0.752 (0.626 - 1)	0.054
	Gamma	Pre-post	0.759 (0.648 - 1)	50.7%
		Slope	0.677 (0.568 - 1)	0.110
F3	Theta	Pre-post	0.629 (0.515 - 1)	86.1%
		Slope	0.718 (0.603 - 1)	0.134
	Alpha	Pre-post	0.723 (0.593 - 1)	52.1%
		Slope	0.706 (0.592 - 1)	0.078
	Beta	Pre-post	0.761 (0.658 - 1)	25.1%

		Slope	0.797 (0.686 - 1)	0.054
	Gamma	Pre-post	0.803 (0.671 - 1)	34.3%
		Slope	0.631 (0.529 - 1)	0.122
C4	Theta	Pre-post	0.729 (0.604 - 1)	49.5%
		Slope	0.655 (0.559 - 1)	0.138
	Alpha	Pre-post	0.747 (0.621 - 1)	46.9%
		Slope	0.710 (0.595 - 1)	0.104
	Beta	Pre-post	0.722 (0.605 - 1)	73.7%
		Slope	0.735 (0.606 - 1)	0.071
	Gamma	Pre-post	0.773 (0.634 - 1)	58.7%
		Slope	0.760 (0.634 - 1)	0.110
C3	Theta	Pre-post	0.878 (0.783 - 1)	49.8%
		Slope	0.771 (0.655 - 1)	0.010
	Alpha	Pre-post	0.682 (0.553 - 1)	47.7%
		Slope	0.619 (0.507 - 1)	0.078
	Beta	Pre-post	0.678 (0.565 - 1)	37.7%
		Slope	0.701 (0.583 - 1)	0.078
	Gamma	Pre-post	0.740 (0.618 - 1)	47.0%
		Slope	0.692 (0.567 - 1)	0.078

303 ICC, intraclass correlation coefficient; CI, confidence interval; SEM, standard error of
304 measurement

305

306 ***Electromyography***

The change in RMS across blocks also showed a similar pattern in both sessions. In the knee flexors, there was a significant effect of the block factor, with a decrease in BF ($p=0.003$, $\eta_p^2=0.30$, power=0.91) and ST ($p < 0.001$, $\eta_p^2=0.43$, power >0.99) amplitude. Post-hoc testing revealed significant differences between the first and fifth and sixth blocks for the BF and between the first and fifth to eighth blocks for the ST. Conversely, there was no significant effect of the block factor in the normalized RMS of the knee extensors (p=0.144 to 0.584). There were also no significant block × session interactions for the flexor (p=0.392 to 0.757) and extensor (p=0.298 to 0.766) muscles (Figure 4).

Table 4. EMG variables test-retest ICC and SEM

EMG variable	Parameter	Test-retest ICC (95% CI)	Test-retest SEM
VL	Pre-post	0.722 (0.583 - 1)	29.5%
	Slope	0.623 (0.531 - 1)	0.083
RF	Pre-post	0.784 (0.686 - 1)	26.2%
	Slope	0.787 (0.675 - 1)	0.034
VM	Pre-post	0.767 (0.664 - 1)	25.5%
	Slope	0.728 (0.614 - 1)	0.044
BF	Pre-post	0.790 (0.680 - 1)	15.1%
	Slope	0.792 (0.685 - 1)	0.025
ST	Pre-post	0.727 (0.623 - 1)	11.4%
	Slope	0.656 (0.573 - 1)	0.020
CCI_{lat}	Pre-post	0.653 (0.551 - 1)	31.5%
	Slope	0.728 (0.583 - 1)	0.799
CCI_{med}	Pre-post	0.693 (0.576 - 1)	34.1%
	Slope	0.715 (0.596 - 1)	1.056

ICC, intraclass correlation coefficient; CI, confidence interval; SEM, standard error of measurement

As for the cocontraction indices, CCI_{lat} showed a significant effect of the block factor ($p=0.001$, $\eta_p^2=0.375$, power=0.97). Post-hoc testing revealed that there was a significant increase from the second to the fourth to eighth blocks. On the contrary, despite the positive slope, CCI_{med} showed no significant changes during the task ($p=0.092$). There were also no significant block × session interactions ($p=0.550$ to 0.799) (Figure 4). The EMG and CCI nonparametric concordance coefficients ranged from 0.65 to 0.79 for the percentage of change from the first to the last block and from 0.62 to 0.80 (both moderate to good) for the slope of the changes over the eight blocks (Table 4). There were no significant between-session differences in any of the EMG variables ($p=0.29$ to 0.894).

Corticomuscular coherence

There was a significant effect of the block factor for the area of significant CMC, with a decrease in all muscles (VL: $p=0.002$, $\eta_p^2=0.324$, power=0.94; RF: $p=0.003$, $\eta_p^2=0.268$, power=0.93; VM: $p < 0.001$, $\eta_p^2=0.302$, power=0.98; BF: $p < 0.001$, $\eta_p^2=0.392$, power=0.99; ST: $p < 0.001$, $\eta_p^2=0.374$, power=0.98). The results of post-hoc testing can be seen in figure 5; these differences tended to show lower CMC in the second half of the task. There was also a significant effect of the session factor for all muscles, with higher values in session 2 (VL: $p=0.001$, $\eta_p^2=0.624$, power=0.97; RF: $p < 0.001$, $\eta_p^2=0.715$, power >0.99; VM: $p < 0.001$, $\eta_p^2=0.674$, power=0.99; BF: $p < 0.001$, $\eta_p^2=0.392$, power=0.99; ST: $p < 0.001$, $\eta_p^2=0.374$, power=0.98). There were no significant block × session interactions for any EEG-EMG pair ($p=0.285$ to 0.813). Regarding the test-retest analysis, the significant coherence area nonparametric concordance coefficients ranged from 0.683 to 0.790 for the pre-post differences and from 0.667 to 0.814 (both moderate to good) for the slope of the change during the task (Table 5).

Table 5. Corticomuscular coherence test-retest ICC and SEM

Coherence pair	Parameter	Test-retest ICC (95% CI)	Test-retest SEM
C3-VL	Pre-post	0.702 (0.577 - 1)	18.4%
	Slope	0.667 (0.551 - 1)	1365
C3-RF	Pre-post	0.728 (0.621 - 1)	23.4%
	Slope	0.775 (0.659 - 1)	1120
C3-VM	Pre-post	0.790 (0.683 - 1)	16.1%
	Slope	0.814 (0.714 - 1)	966
C3-BF	Pre-post	0.726 (0.626 - 1)	17.6%

	Slope	0.743 (0.633 - 1)	1140
C3-ST	Pre-post	0.771 (0.657 - 1)	12.6%
	Slope	0.781 (0.657 - 1)	787

ICC, intraclass correlation coefficient; CI, confidence interval; SEM, standard error of measurement

The first block images in the time-frequency CMC maps (Figure 6) show two zones with the highest absolute values, located around 3 and 6-8 Hz. While the 3-Hz CMC generally manifested from 4-6 s, the 6-8 Hz CMC was frequently present throughout the entire 8-s period. In line with the significant coherence analysis, a generalized decrease in absolute CMC can be observed from the first to the last block, especially in the frequency zones mentioned above.

Discussion

Knee movement rate significantly decreased until half of task duration followed by a plateau until the end. In association with this decrease, we found both central and peripheral electrophysiological changes. There were significant decreases in normalized EEG power, especially at the frontal electrodes, while the CMC analysis showed a decrease in brain-muscle functional coupling during the task. EMG testing revealed a decrease in knee flexor normalized RMS and increased VL/BF co-contraction after the second block.

The degree of knee motor slowing was similar to what we previously observed in a preliminary study (17). The loss of movement rate (-15.8% and -12.9% in the two sessions) is comparable, albeit slightly lower, than what has been observed in finger tapping tasks of 10-30 s in total (18-27%)(2–4) and closer to similar periods of foot tapping (~15%)(1, 38), despite the difference in task parameters. Considering the longer duration of our task (8 blocks of 10 s vs. a single 10-30 s period in the cited studies), a greater loss could be expected. However, unlike we hypothesized, the movement rate decreased only until the fourth block (i.e., 55 s). Nevertheless, the good to excellent movement rate ICCs and the standard errors of measurement indicate these measures' between-session stability. Comparatively, finger motor slowing has been found to plateau only after about 120 s of continuous tapping, corresponding to a 40% decrease in movement rate (39). Knee motor slowing thus seems to show some similar and some different properties relatively to smaller joints. On one hand, the plateau in knee movement rate was reached at a lower percentage of decrease (13-16% and 25-40% for the knee and fingers, respectively). On the other hand, the trajectory of decrease shows similarities, with a steep decrease in the first stages of the task and a gradual smoothing until a plateau at around 50% of task duration (for comparison, please see (1, 39)). The larger segment inertia may play a role in these differences. While small joint all-out repetitive movement does not present a significant metabolic and homeostatic challenge, our task has greater muscle work and energy demands due to the

larger mass being moved, which may have led to a plateau at a lower percentage of performance loss in order to ensure homeostatic regulation. Interestingly, the ATP-PCr system's contribution during maximal exercise starts plateauing at about 50 seconds (40), which corresponds approximately to the point where the movement rate stabilized in our task. Therefore, energy availability and homeostatic regulation may have played a role in movement rate stabilization after the fourth block.

EEG findings partly support this role of homeostatic regulation. After an initial increase, there was a decrease in EEG power which started even before the movement rate stabilized. Post-hoc testing showed that individual inter-block decreases were seen most commonly between an initial peak at the second or third block (i.e., with low fatigue but when movement rate was decreasing) and lower values within the second half of the task (i.e., with greater fatigue but stable movement rate). It has been reported that brain activity increases with fatigue or task demands (41–44); this increased central drive aims to compensate for the decreased peripheral ability to produce force. Our opposing findings may be due to inhibitory activity of group III/IV sensory afferents, whose involvement in both central and peripheral fatigue development has previously been reported (45, 46). These afferent signals modulate motoneuron output, leading to decreased muscle activation (45). Although speculative, this explanation is supported by our EEG and flexor EMG findings. Supraspinal performance modulation even before task failure or a performance plateau has also been seen in other tasks (42, 47).

There was a similar EEG trajectory during the task across frequency bands and electrodes, characterized by an initial increase (up to block 2-3) followed by a decrease (until block 4-6), more notably at frontal than at central electrodes. Frontal electrodes cover areas such as the prefrontal and the anterior cingulate cortices, which play a role in movement planning and regulation (48, 49), while central electrodes cover the supplementary motor area and the motor cortex, which are involved in the temporal coding of movement parameters and in producing the descending motor command (50, 51). EEG data thus show that movement planning may have been more affected by our task than the production of the motor command. Additionally, the significant effect of the block factor in all frequency bands at frontal electrodes contributes to the growing evidence that the cortex plays a significant role in rhythmic movement control (41, 50, 52), in this case, performed at maximum speed.

There were no significant changes in knee extensor EMG. Conversely, both the BF and ST normalized RMS significantly decreased continuously throughout the task despite the movement rate stabilization after the fourth block. These differences between flexors and extensors were probably due to the anti-gravity position of knee flexion in our task. Other studies of maximal lower limb intermittent effort have also found a continuous decrease in EMG amplitude throughout the task (53–56). The decrease in knee flexor EMG amplitude may be caused by selective fatigue of fast-twitch fibers, since these have been shown to be preferentially recruited during rapid contractions (57, 58). It makes sense that the number of motor units sufficiently fast to cope with the movement rate demands decreased continuously during the task, thus explaining the generally continuous decrease in normalized RMS in our study. Considering the changes in EEG power, impaired central recruitment could also be the cause of the flexor EMG amplitude decrease. However, if this was the case, there should not be a continuous decline in EMG amplitude, and it is also not in line with the plateau in movement rate.

Previous studies have found an increase in muscle half relaxation time(3, 59), a loss of a clear agonist-antagonist EMG pattern after fatiguing finger tapping tasks(2), and a decrease in the agonist-antagonist activation delay in a cycling repeated sprinting task(60). In our study, the fact that CCI_{lat} increased gradually from the second block despite the decrease in BF RMS further suggests a greater temporal agonist-antagonist overlap with increasing fatigue, as previously reported(2). This increased overlap may be due to the earlier fatigability of fast-twitch fibers, which would lead to prolonged muscle activation in order to maintain movement rate(57, 58). It is logical that this greater EMG overlap/co-contraction and lower availability of fast muscle fibers would lead to a decrease in movement rate; however, in that case, both CCIs should not have continued to increase during the second half of the task. Thus, it seems the continuously worsening EMG overlap with fatigue did not impair movement rate after a certain point. It is also noteworthy that the CCIs continued to increase despite the lack of changes in EEG power, indicating that this was not due to the strength of the central drive. It may therefore be more related to the quality of the motor command than to its intensity, which may be corroborated by the CMC findings discussed below.

There was a decrease in the area of significant CMC in all muscles, reflecting a generalized loss of brain-muscle coupling, which in turn was associated with the decreased movement rate. It is interesting to note that despite the lack of significant changes in knee extensor normalized EMG amplitude, there was still a loss of knee extensor CMC, suggesting that decoupling may occur even in the absence of significant EMG amplitude changes. This may be a sign of a centrally driven generalized loss of coupling between brain and muscle activity during the task, perhaps due to the breakdown of central motor control mechanisms related to the change in movement direction caused by unsustainable task demands suggested by Rodrigues et al.(2).

There were two frequency zones of higher CMC in the first block (around 3 and 6-8 Hz). These two zones may represent the movement rate (fundamental frequency, F0) and its first harmonic (F1) frequency. Previous studies of both hand and feet rhythmic movements also found stronger coherence at these two frequencies (50, 61). Our task caused a greater decrease in F0 than in F1. It is worth noting that these two frequencies are generated by different cortical regions; while F0 is associated with sensorimotor movement kinematics encoding, F1 has been found to be more prominent in the prefrontal cortex, which is responsible for movement planning, timing, and self-initiation (50, 62). We found greater decreases in the F0 range, suggesting an impairment in movement kinematics encoding, which is consistent with the breakdown of the motor command mentioned as a cause of motor slowing mentioned previously (2). Thus, isolated EEG changes suggest that movement planning areas are more affected by the task, but CMC losses seem to be more related to the motor command.

Whether maximal exercise performance is regulated to limit the development of catastrophic fatigue remains controversial (63, 64). Here, a plateau of performance was reached at about 50% of task duration. Early performance decreases followed by a plateau until task completion have been seen in distinct maximal effort upper and lower limb joint tasks (39, 42, 53, 54, 56, 63), suggesting the presence of some common regulation mechanism. Nevertheless, the percentage of decrease in performance at which this plateau is reached is task-dependent (1, 39, 63). Our findings suggest that performance was regulated in the

absence of catastrophic failure but not exclusively due to peripheral feedback; rather, it seems that multiple systems may have influenced the central motor command and limit further decreases in exercise performance. The level of task performance decrease before this plateau is reached may therefore be both task- and system- (i.e., locomotor, cardiometabolic) specific. Naturally, this requires further confirmation.

Limitations

Despite our attempts to monitor processes from the brain to the motor output, some limitations remain. We did not obtain EMG data from both limbs or from other muscles which may have played a role in our task (e.g., gastrocnemius). However, since our participants were healthy and the task was bilaterally symmetrical, we did not anticipate significant between-limb differences. We also did not measure fatigue perception, which limits our discussion of task demands. Moreover, the highly dynamic nature of our task means that despite our best efforts to clean the EEG signal, some degree of noise can still be expected, considering the difficult balance between signal cleaning and loss of physiological information. Our findings may also not be generalizable to female participants or other age groups. Finally, although all individuals had at least a week between sessions, the length of this interval was not uniform.

Conclusions

The designed task was able to induce significant knee motor slowing, but this decrease in movement rate stopped halfway through the task. Electrophysiological data suggest that both central and peripheral processes were involved in this slowing. Most notably, we found a decrease in EEG power after an initial peak, followed by a subsequent stabilization, while there was a continuous decrease in flexor EMG activity and increase in co-contraction. CMC decreased during the task, suggesting an impairment of EEG-EMG functional coupling with fatigue. However, no single analysis showed an isolated direct relation with task performance, suggesting that the interaction of changes at various levels was involved in performance regulation.

Statements and declarations

Author contributions

Conceptualization: José Pedro Correia, João R. Vaz, Sandro R. Freitas; Methodology: José Pedro Correia, João R. Vaz, Sandro R. Freitas; Formal analysis and investigation: José Pedro Correia, Christophe Domingos, Pedro Luís; Writing - original draft preparation: José Pedro Correia; Writing - review and editing: all authors; Resources: Agostinho Rosa, Sandro R. Freitas; Supervision: Erik Witvrouw, João R. Vaz, Sandro R. Freitas

Compliance with Ethical Standards

Research involving Human Participants and/or Animals: The study was performed according to recommendations of the Declaration of Helsinki and was approved by the local institutional review board (approval number: 8/2021).

Informed consent: All participants provided written informed consent.

Competing interests: The authors declare that they have no competing interests.

Data availability statement: The datasets generated during and/or analyzed during the current study are available from the corresponding author on reasonable request.

References

1. **Bächinger M**, **Lehner R**, **Thomas F**, **Hanimann S**, **Balsters J**, **Wenderoth N**. Human motor fatigability as evoked by repetitive movements results from a gradual breakdown of surround inhibition. *Elife* 8, 2019. doi: 10.7554/eLife.46750.

2. **Rodrigues JP**, **Mastaglia FL**, **Thickbroom GW**. Rapid slowing of maximal finger movement rate: fatigue of central motor control? *Exp Brain Res* 196: 557–563, 2009.

3. **Madrid A**, **Madinabeitia-Mancebo E**, **Cudeiro J**, **Arias P**. Effects of a Finger Tapping Fatiguing Task on M1-Intracortical Inhibition and Central Drive to the Muscle. *Sci Rep* 8: 9326, 2018.

4. **Arias P**, **Robles-García V**, **Corral-Bergantiños Y**, **Madrid A**, **Espinosa N**, **Valls-Solé J**, **Grieve KL**, **Oliviero A**, **Cudeiro J**. Central fatigue induced by short-lasting finger tapping and isometric tasks: A study of silent periods evoked at spinal and supraspinal levels. *Neuroscience* 305: 316–327, 2015.

5. **Zanette G**, **Bonato C**, **Polo A**, **Tinazzi M**, **Manganotti P**, **Fiaschi A**. Long-lasting depression of motor-evoked potentials to transcranial magnetic stimulation following exercise. *Exp Brain Res* 107: 80–86, 1995.

6. **Pfann KD**, **Hoffman DS**, **Gottlieb GL**, **Strick PL**, **Corcos DM**. Common principles underlying the control of rapid, single degree-of-freedom movements at different joints. *Exp Brain Res* 118: 35–51, 1998.

7. **Freund HJ**, **Büdingen HJ**. The relationship between speed and amplitude of the fastest voluntary contractions of human arm muscles. *Exp Brain Res* 31: 1–12, 1978.

8. **Grosse P**, **Cassidy MJ**, **Brown P**. EEG–EMG, MEG–EMG and EMG–EMG frequency analysis: physiological principles and clinical applications. *Clinical Neurophysiology* 113: 1523–1531, 2002.

9. **Luft AR**, **Smith GV**, **Forrester L**, **Whitall J**, **Macko RF**, **Hauser T-K**, **Goldberg AP**, **Hanley DF**. Comparing brain activation associated with isolated upper and lower limb movement across corresponding joints. *Hum Brain Mapp* 17: 131–140, 2002.

10. **Kapreli E**, **Athanasopoulos S**, **Papathanasiou M**, **Van Hecke P**, **Strimpakos N**, **Gouliamos A**, **Peeters R**, **Sunaert S**. Lateralization of brain activity during lower limb

joints movement. An fMRI study. *Neuroimage* 32: 1709–1721, 2006.

11. **Kapreli E**, **Athanasopoulos S**, **Papathanasiou M**, **Van Hecke P**, **Keleki D**, **Peeters R**, **Strimpakos N**, **Sunaert S**. Lower limb sensorimotor network: issues of somatotopy and overlap. *Cortex* 43: 219–232, 2007.

12. **Chéron G**, **Godaux E**. Self-terminated fast movement of the forearm in man: amplitude dependence of the triple burst pattern. *J Med Nucl Biophys* 10: 109–117, 1986.

13. **Benecke R**, **Meinck HM**, **Conrad B**. Rapid goal-directed elbow flexion movements: limitations of the speed control system due to neural constraints. *Exp Brain Res* 59: 470–477, 1985.

14. **Goel R**, **Paloski WH**. Motor Control Performance During Rapid Voluntary Movements of Elbow and Knee. *J Mot Behav* 48: 348–356, 2016.

15. **Vernillo G**, **Temesi J**, **Martin M**, **Krüger RL**, **Millet GY**. Spinal contribution to neuromuscular recovery differs between elbow-flexor and knee-extensor muscles after a maximal sustained fatiguing task. *J Neurophysiol* 124: 763–773, 2020.

16. **Temesi J**, **Vernillo G**, **Martin M**, **Krüger RL**, **McNeil CJ**, **Millet GY**. Sustained Maximal Voluntary Contractions Elicit Different Neurophysiological Responses in Upper- and Lower-Limb Muscles in Men. *Neuroscience* 422: 88–98, 2019.

17. **Correia JP**, **Vaz JR**, **Witvrouw E**, **Freitas SR**. Range of Motion Remains Constant as Movement Rate Decreases During a Repetitive High-Speed Knee Flexion-Extension Task. *Motor Control* 26: 465–476, 2022.

18. **Hubel KA**, **Reed B**, **Yund EW**, **Herron TJ**, **Woods DL**. Computerized measures of finger tapping: effects of hand dominance, age, and sex. *Percept Mot Skills* 116: 929–952, 2013.

19. **Laurent CM**, **Green JM**, **Bishop PA**, **Sjökvist J**, **Schumacker RE**, **Richardson MT**, **Curtner-Smith M**. Effect of gender on fatigue and recovery following maximal intensity repeated sprint performance. *J Sports Med Phys Fitness* 50: 243–253, 2010.

20. **Bartzokis G**, **Lu PH**, **Tingus K**, **Mendez MF**, **Richard A**, **Peters DG**, **Oluwadara B**, **Barrall KA**, **Finn JP**, **Villablanca P**, **Thompson PM**, **Mintz J**. Lifespan trajectory of myelin integrity and maximum motor speed. *Neurobiol Aging* 31: 1554–1562, 2010.

21. **Wieser M**, **Haefeli J**, **Bütler L**, **Jäncke L**, **Riener R**, **Koeneke S**. Temporal and spatial patterns of cortical activation during assisted lower limb movement. *Exp Brain Res* 203: 181–191, 2010.

22. **Hermens HJ**, **Freriks B**, **Disselhorst-Klug C**, **Rau G**. Development of recommendations for SEMG sensors and sensor placement procedures. *J Electromyogr Kinesiol* 10: 361–374, 2000.

23. **Yoshida T**, **Masani K**, **Zabjek K**, **Chen R**, **Popovic MR**. Dynamic Increase in Corticomuscular Coherence during Bilateral, Cyclical Ankle Movements. *Front Hum Neurosci* 11: 155, 2017.

24. **Yoshida T**, **Masani K**, **Zabjek K**, **Chen R**, **Popovic MR**. Dynamic cortical participation during bilateral, cyclical ankle movements: effects of aging. *Sci Rep* 7: 44658, 2017.

25. **Nalçaci E**, **Kalaycioğlu C**, **Ciçek M**, **Genç Y**. The relationship between handedness and fine motor performance. *Cortex* 37: 493–500, 2001.

26. **Agnew JA**, **Zeffiro TA**, **Eden GF**. Left hemisphere specialization for the control of voluntary movement rate. *Neuroimage* 22: 289–303, 2004.

27. **Hervé P-Y**, **Mazoyer B**, **Crivello F**, **Perchey G**, **Tzourio-Mazoyer N**. Finger tapping, handedness and grey matter amount in the Rolando's genu area. *NeuroImage* 25: 1133–1145, 2005.

28. **Delorme A**, **Makeig S**. EEGLAB: an open source toolbox for analysis of single-trial EEG dynamics including independent component analysis. *Journal of Neuroscience Methods* 134: 9–21, 2004.

29. **Mima T**, **Steger J**, **Schulman AE**, **Gerloff C**, **Hallett M**. Electroencephalographic measurement of motor cortex control of muscle activity in humans. *Clin Neurophysiol* 111: 326–337, 2000.

30. **Ball N**, **Scurr J**. Electromyography normalization methods for high-velocity muscle actions: review and recommendations. *J Appl Biomech* 29: 600–608, 2013.

31. **Lo J**, **Lo O-Y**, **Olson EA**, **Habtemariam D**, **Iloputaife I**, **Gagnon MM**, **Manor B**, **Lipsitz LA**. Functional implications of muscle co-contraction during gait in advanced age. *Gait Posture* 53: 110–114, 2017.

32. **Liu J**, **Sheng Y**, **Zeng J**, **Liu H**. Corticomuscular Coherence for Upper Arm Flexor and Extensor Muscles During Isometric Exercise and Cyclically Isokinetic Movement. *Front Neurosci* 13: 522, 2019.

33. **Cohen J**. *Statistical Power Analysis for the Behavioral Sciences*. Routledge, 2013.

34. **Koo TK**, **Li MY**. A Guideline of Selecting and Reporting Intraclass Correlation Coefficients for Reliability Research. *J Chiropr Med* 15: 155–163, 2016.

35. **Bobak CA**, **Barr PJ**, **O'Malley AJ**. Estimation of an inter-rater intra-class correlation coefficient that overcomes common assumption violations in the assessment of health measurement scales. *BMC Med Res Methodol* 18: 93, 2018.

36. **Kuiper R**, **Hogenboezem R**. nopaco: a non-parametric concordance coefficient [Online]. 2017. https://cran.microsoft.com/snapshot/2018-07-26/web/packages/nopaco/vignettes/nopaco.pdf [27 Dec. 2022].

37. **Weir JP**. QUANTIFYING TEST-RETEST RELIABILITY USING THE INTRACLASS CORRELATION COEFFICIENT AND THE SEM. *Journal of Strength and Conditioning Research* 19: 231–240, 2005.

38. **Seidel-Marzi O**, **Ragert P**. Anodal transcranial direct current stimulation reduces motor slowing in athletes and non-athletes. *BMC Neurosci* 21: 26, 2020.

39. **Madinabeitia-Mancebo E**, **Madrid A**, **Jácome A**, **Cudeiro J**, **Arias P**. Temporal dynamics of muscle, spinal and cortical excitability and their association with kinematics during three minutes of maximal-rate finger tapping. *Sci Rep* 10: 3166, 2020.

40. **Gastin PB**. Energy system interaction and relative contribution during maximal exercise. *Sports Med* 31: 725–741, 2001.

41. **Enders H**, **Cortese F**, **Maurer C**, **Baltich J**, **Protzner AB**, **Nigg BM**. Changes in cortical activity measured with EEG during a high-intensity cycling exercise. *J Neurophysiol* 115: 379–388, 2016.

42. **Liu JZ**, **Dai TH**, **Sahgal V**, **Brown RW**, **Yue GH**. Nonlinear cortical modulation of muscle fatigue: a functional MRI study. *Brain Res* 957: 320–329, 2002.

43. **Liu JZ**, **Shan ZY**, **Zhang LD**, **Sahgal V**, **Brown RW**, **Yue GH**. Human brain activation during sustained and intermittent submaximal fatigue muscle contractions: an FMRI study. *J Neurophysiol* 90: 300–312, 2003.

44. **Bailey SP**, **Hall EE**, **Folger SE**, **Miller PC**. Changes in EEG during graded exercise on a recumbent cycle ergometer. *J Sports Sci Med* 7: 505–511, 2008.

45. **Amann M**, **Sidhu SK**, **Weavil JC**, **Mangum TS**, **Venturelli M**. Autonomic responses to exercise: group III/IV muscle afferents and fatigue. *Auton Neurosci* 188: 19–23, 2015.

46. **Sidhu SK**, **Weavil JC**, **Thurston TS**, **Rosenberger D**, **Jessop JE**, **Wang E**, **Richardson RS**, **McNeil CJ**, **Amann M**. Fatigue-related group III/IV muscle afferent feedback facilitates intracortical inhibition during locomotor exercise. *J Physiol* 596: 4789–4801, 2018.

47. **Rupp T**, **Perrey S**. Prefrontal cortex oxygenation and neuromuscular responses to exhaustive exercise. *Eur J Appl Physiol* 102: 153–163, 2008.

48. **Scott SH**. Optimal feedback control and the neural basis of volitional motor control. *Nat Rev Neurosci* 5: 532–546, 2004.

49. **Herz DM**, **Tan H**, **Brittain J-S**, **Fischer P**, **Cheeran B**, **Green AL**, **FitzGerald J**, **Aziz TZ**, **Ashkan K**, **Little S**, **Foltynie T**, **Limousin P**, **Zrinzo L**, **Bogacz R**, **Brown P**. Distinct mechanisms mediate speed-accuracy adjustments in cortico-subthalamic networks. *Elife* 6, 2017. doi: 10.7554/eLife.21481.

50. **Bourguignon M**, **Jousmäki V**, **Op de Beeck M**, **Van Bogaert P**, **Goldman S**, **De Tiège X**. Neuronal network coherent with hand kinematics during fast repetitive hand movements. *Neuroimage* 59: 1684–1691, 2012.

51. **Loh KK**, **Hadj-Bouziane F**, **Petrides M**, **Procyk E**, **Amiez C**. Rostro-Caudal Organization of Connectivity between Cingulate Motor Areas and Lateral Frontal Regions. *Front Neurosci* 11: 753, 2017.

52. **Jain S**, **Gourab K**, **Schindler-Ivens S**, **Schmit BD**. EEG during pedaling: evidence for cortical control of locomotor tasks. *Clin Neurophysiol* 124: 379–390, 2013.

53. **Mendez-Villanueva A**, **Edge J**, **Suriano R**, **Hamer P**, **Bishop D**. The recovery of repeated-sprint exercise is associated with PCr resynthesis, while muscle pH and EMG amplitude remain depressed. *PLoS One* 7: e51977, 2012.

54. **Mendez-Villanueva A**, **Hamer P**, **Bishop D**. Fatigue in repeated-sprint exercise is related to muscle power factors and reduced neuromuscular activity. *Eur J Appl Physiol* 103: 411–419, 2008.

55. **Billaut F**, **Smith K**. Prolonged repeated-sprint ability is related to arterial O2 desaturation in men. *Int J Sports Physiol Perform* 5: 197–209, 2010.

56. **Brocherie F**, **Millet GP**, **Girard O**. Neuro-mechanical and metabolic adjustments to the repeated anaerobic sprint test in professional football players. *Eur J Appl Physiol* 115: 891–903, 2015.

57. **Wakeling JM**, **Uehli K**, **Rozitis AI**. Muscle fibre recruitment can respond to the mechanics of the muscle contraction. *J R Soc Interface* 3: 533–544, 2006.

58. **Hodson-Tole EF**, **Wakeling JM**. Motor unit recruitment patterns 1: responses to changes in locomotor velocity and incline. *J Exp Biol* 211: 1882–1892, 2008.

59. **Madinabeitia-Mancebo E**, **Madrid A**, **Oliviero A**, **Cudeiro J**, **Arias P**. Peripheral-central interplay for fatiguing unresisted repetitive movements: a study using muscle ischaemia and M1 neuromodulation. *Sci Rep* 11: 2075, 2021.

60. **Billaut F**, **Basset FA**, **Falgairette G**. Muscle coordination changes during intermittent cycling sprints. *Neurosci Lett* 380: 265–269, 2005.

61. **Raethjen J**, **Govindan RB**, **Binder S**, **Zeuner KE**, **Deuschl G**, **Stolze H**. Cortical representation of rhythmic foot movements. *Brain Res* 1236: 79–84, 2008.

62. **Abe M**, **Hanakawa T**. Functional coupling underlying motor and cognitive functions of the dorsal premotor cortex. *Behav Brain Res* 198: 13–23, 2009.

63. **Hureau TJ**, **Olivier N**, **Millet GY**, **Meste O**, **Blain GM**. Exercise performance is regulated during repeated sprints to limit the development of peripheral fatigue beyond a critical threshold. *Exp Physiol* 99: 951–963, 2014.

64. **Thomas K**, **Goodall S**, **Howatson G**. Performance Fatigability Is Not Regulated to A Peripheral Critical Threshold. *Exercise and Sport Sciences Reviews* 46: 240–246, 2018.

Figure legends

Fig. 1. Depiction of the experimental setup along with raw data from each analysis. VL, vastus lateralis; RF, rectus femoris; VM, vastus medialis; BF, biceps femoris; ST, semitendinosus.

Fig. 2. Decreases in movement rate during the task. The shaded areas represent the 95% confidence interval for the first (blue) and second (orange) sessions. *significantly different from the first block ($p < 0.05$). **significantly different from the first three blocks ($p < 0.05$). These significant differences were seen in the 2×8 repeated measures ANOVA post-hoc multiple comparisons.

Fig. 3. Changes in normalized EEG power during the task. Most electrodes with significant differences show an increase until block 2-3, followed by a decrease until block 4-6. The shaded areas represent the 95% confidence interval for the first (blue) and second (orange) sessions. *significant difference from the first block ($p < 0.05$); **significant difference from the second block ($p < 0.05$): ***significant difference from the third block ($p < 0.05$). These significant differences were seen in the 2×8 repeated measures ANOVA post-hoc multiple comparisons.

Fig. 4. Normalized root mean square (RMS) and co-contraction indices during the task, showing a significant decrease in flexor amplitude and increase in co-contraction. The shaded areas represent the 95% confidence interval for the first (blue) and second (orange) sessions. VL, vastus lateralis; RF, rectus femoris; VM, vastus medialis; BF, biceps femoris; ST, semitendinosus; CCI_{lat}, lateral co-contraction index; CCI_{med}, medial co-contraction index

*significantly different from the first block ($p < 0.05$); **significantly different from the second block ($p < 0.05$). These significant differences were seen in the 2×8 repeated measures ANOVA post-hoc multiple comparisons.

Fig. 5. Decreases in the area of significant coherence during the task. The shaded areas represent the 95% confidence interval for the first (blue) and second (orange) sessions. AU, arbitrary units; VL, vastus lateralis; RF, rectus femoris; VM, vastus medialis; BF, biceps femoris; ST, semitendinosus. *significantly different from the first block ($p < 0.05$); **significantly different from the second block ($p < 0.05$). These significant differences were seen in the 2×8 repeated measures ANOVA post-hoc multiple comparisons. #, significant difference between sessions ($p < 0.05$, 2×8 repeated measures ANOVA)

Fig. 6. Time-frequency maps of corticomuscular coherence in the first and last blocks between the C3 EEG electrode and each muscle. VL, vastus lateralis; RF, rectus femoris; VM, vastus medialis; BF, biceps femoris; ST, semitendinosus. The color bar represents the range of coherence values.

Supplementary materials

Supplementary file S1. Matlab code files used for data processing

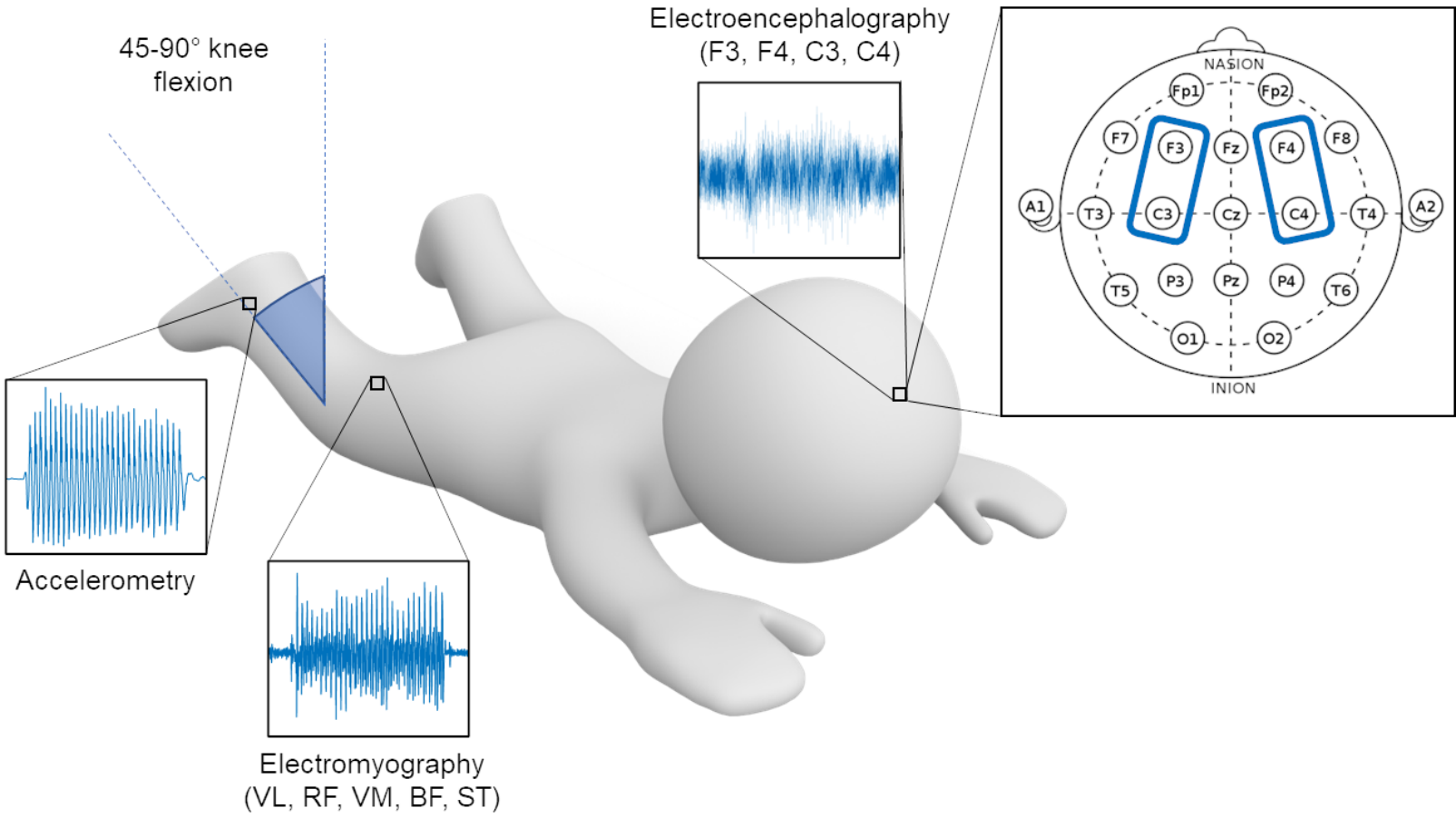
45-90° knee flexion
Electroencephalography (F3, F4, C3, C4)
NASION
Fp1
Fp2
F7
F3
Fz
F4
F8
A1
T3
C3
Cz
C4
T4
A2
T5
P3
Pz
P4
T6
O1
O2
INION
Accelerometry
Electromyography (VL, RF, VM, BF, ST)

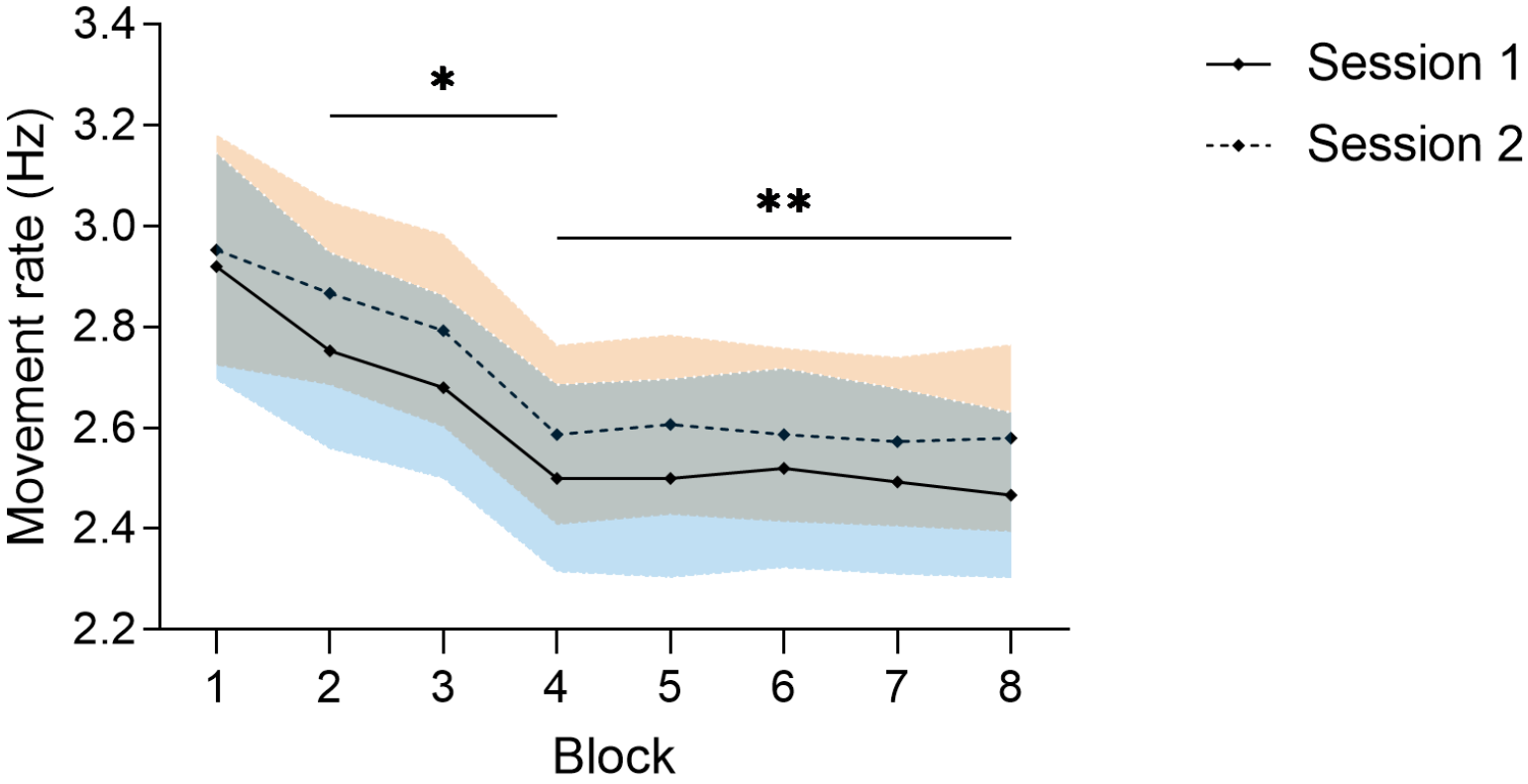
3.4
3.2
3.0
2.8
2.6
2.4
2.2
Movement rate (Hz)
*
**
1
2
3
4
5
6
7
8
Block
Session 1
Session 2

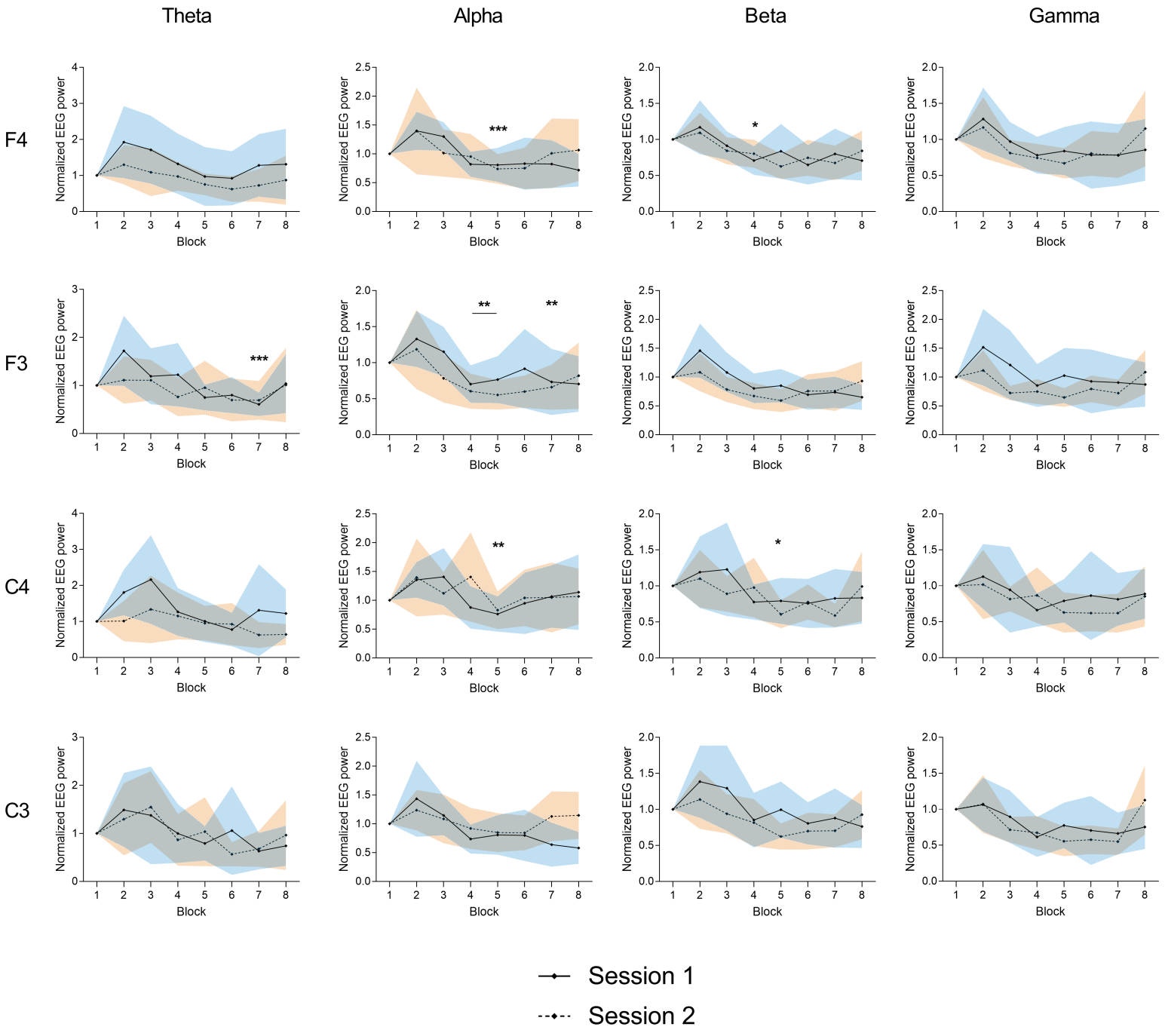
Theta
Alpha
Beta
Gamma
F4
F3
C4
C3
Normalized EEG power
Block
***
**
*
Session 1
Session 2

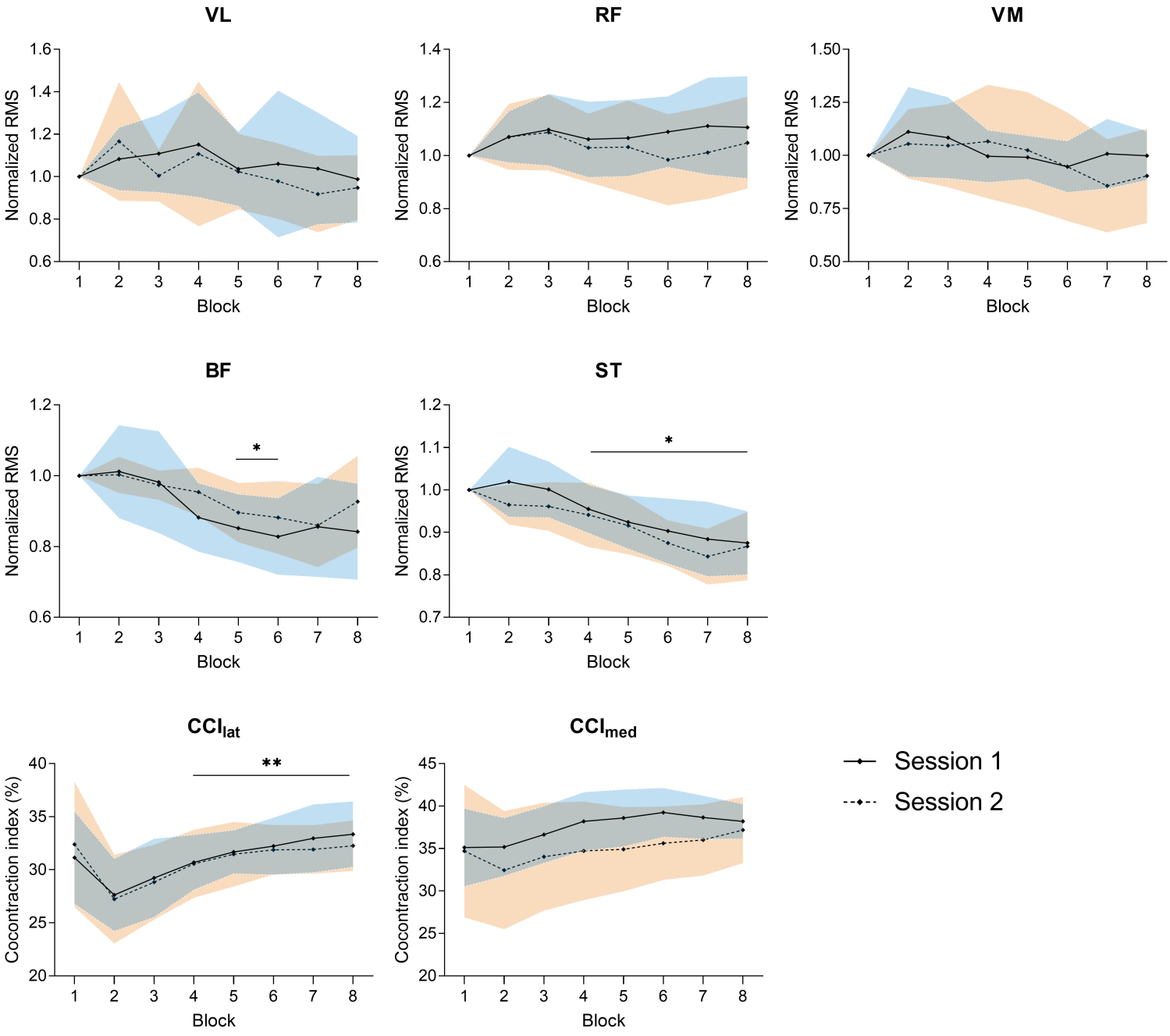
VL
RF
VM
BF
ST
CCI$_{lat}$
CCI$_{med}$
Normalized RMS
Cocontraction index (%)
Block
*
**
Session 1
Session 2

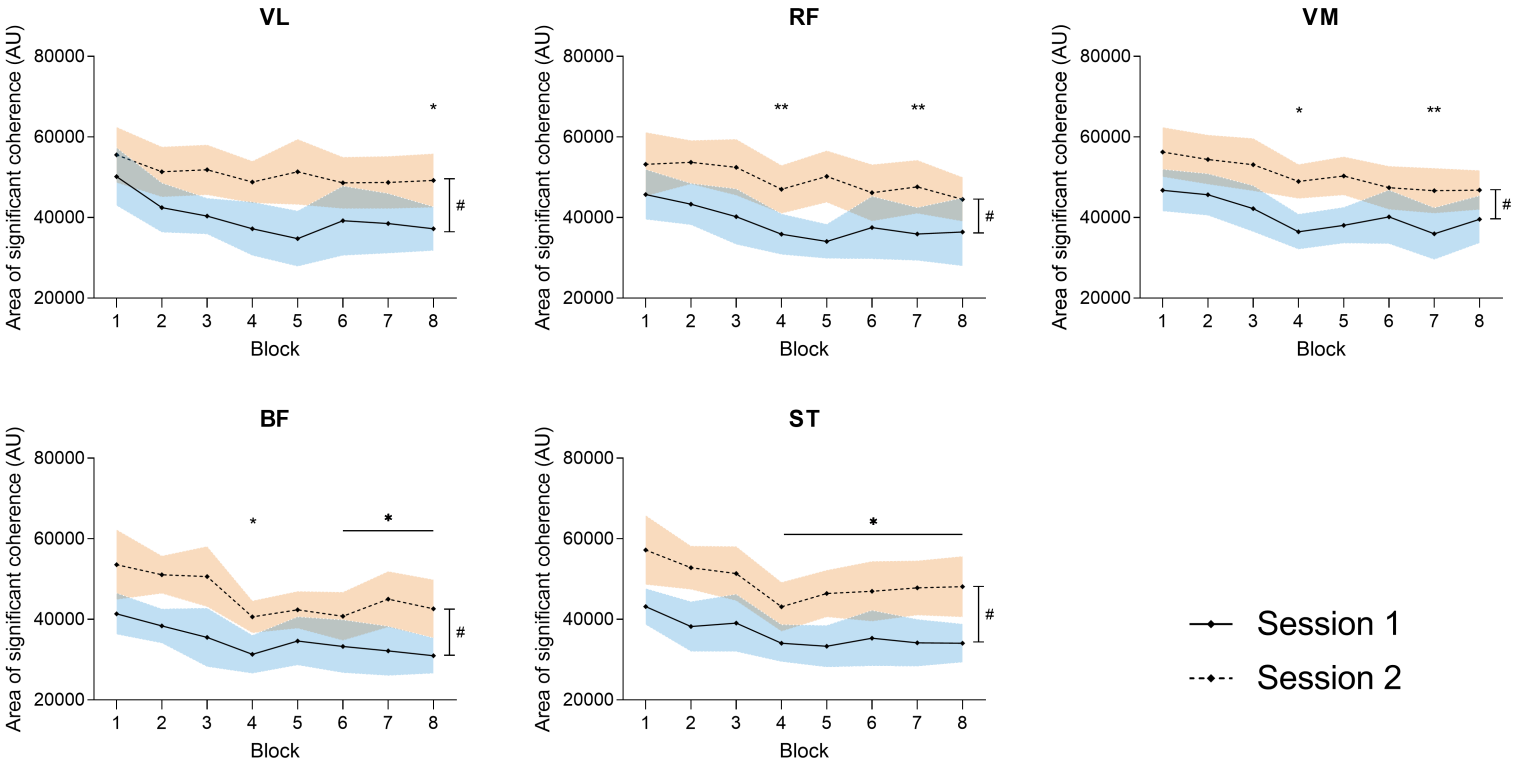
VL
RF
VM
BF
ST
Area of significant coherence (AU)
80000
60000
40000
20000
1
2
3
4
5
6
7
8
Block
*
**
#
Session 1
Session 2

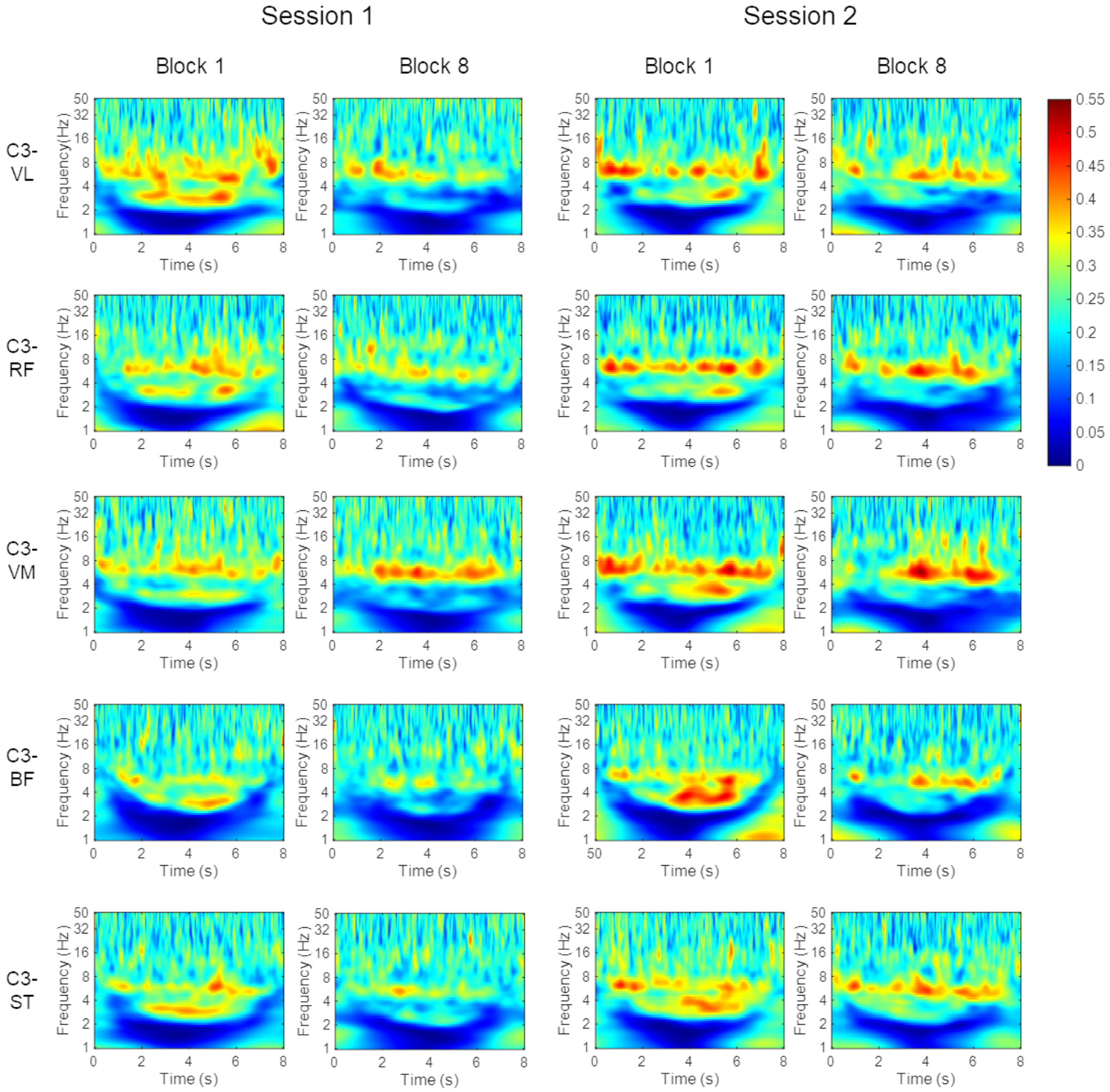
Session 1
Session 2
Block 1
Block 8
Block 1
Block 8
C3-VL
C3-RF
C3-VM
C3-BF
C3-ST
Frequency (Hz)
Time (s)
50
32
16
8
4
2
1
0
2
4
6
8
0.55
0.5
0.45
0.4
0.35
0.3
0.25
0.2
0.15
0.1
0.05
0

Table 1. Movement rate test-retest ICC and SEM

Block	Test-retest ICC (95% CI)	Test-retest SEM (Hz)
1	0.852 (0.559 - 0.95)	0.20
2	0.805 (0.385 - 0.934)	0.16
3	0.891 (0.675 - 0.963)	0.15
4	0.740 (0.291 - 0.908)	0.23
5	0.888 (0.670 - 0.962)	0.14
6	0.915 (0.760 - 0.970)	0.14
7	0.912 (0.754 - 0.969)	0.13
8	0.858 (0.607 - 0.950)	0.16

ICC, intraclass correlation coefficient; CI, confidence interval; SEM, standard error of measurement

Table 2. Relative EEG power test-retest ICC and SEM

EEG channel	Frequency band	Parameter	Test-retest ICC (95% CI)	Test-retest SEM
F4	Theta	Pre-post	0.768 (0.626 - 1)	144.3%
		Slope	0.658 (0.547 - 1)	0.037
	Alpha	Pre-post	0.708 (0.597 - 1)	48.2%
		Slope	0.667 (0.573 - 1)	0.011
	Beta	Pre-post	0.623 (0.532 - 1)	43.4%
		Slope	0.756 (0.642 - 1)	0.016
	Gamma	Pre-post	0.689 (0.568 - 1)	82.2%
		Slope	0.652 (0.562 - 1)	0.008
F3	Theta	Pre-post	0.795 (0.674 - 1)	81.1%
		Slope	0.824 (0.716 - 1)	0.020
	Alpha	Pre-post	0.616 (0.515 - 1)	51.8%
		Slope	0.684 (0.579 - 1)	0.010
	Beta	Pre-post	0.669 (0.562 - 1)	46.0%
		Slope	0.740 (0.641 - 1)	0.010
	Gamma	Pre-post	0.722 (0.604 - 1)	88.3%
		Slope	0.694 (0.591 - 1)	0.010
C4	Theta	Pre-post	0.746 (0.631 - 1)	65.9%
		Slope	0.732 (0.616 - 1)	0.025
	Alpha	Pre-post	0.666 (0.554 - 1)	29.7%
		Slope	0.659 (0.582 - 1)	0.009

	Beta	Pre-post	0.680 (0.569 - 1)	44.9%
		Slope	0.738 (0.615 - 1)	0.013
	Gamma	Pre-post	0.683 (0.574 - 1)	127.7%
		Slope	0.675 (0.573 - 1)	0.015
C3	Theta	Pre-post	0.762 (0.648 - 1)	73.5%
		Slope	0.698 (0.576 - 1)	0.029
	Alpha	Pre-post	0.720 (0.601 - 1)	39.6%
		Slope	0.653 (0.571 - 1)	0.010
	Beta	Pre-post	0.744 (0.623 - 1)	81.7%
		Slope	0.762 (0.642 - 1)	0.014
	Gamma	Pre-post	0.723 (0.598 - 1)	155.1%
		Slope	0.678 (0.555 - 1)	0.009

ICC, intraclass correlation coefficient; CI, confidence interval; SEM, standard error of measurement

Table 3. Normalized EEG power test-retest ICC and SEM

EEG channel	Frequency band	Parameter	Test-retest ICC (95% CI)	Test-retest SEM
F4	Theta	Pre-post	0.642 (0.523 - 1)	60.3%
		Slope	0.712 (0.608 - 1)	0.126
	Alpha	Pre-post	0.724 (0.596 - 1)	49.8%
		Slope	0.738 (0.628 - 1)	0.083
	Beta	Pre-post	0.688 (0.594 - 1)	41.5%
		Slope	0.752 (0.626 - 1)	0.054
	Gamma	Pre-post	0.759 (0.648 - 1)	50.7%
		Slope	0.677 (0.568 - 1)	0.110
F3	Theta	Pre-post	0.629 (0.515 - 1)	86.1%
		Slope	0.718 (0.603 - 1)	0.134
	Alpha	Pre-post	0.723 (0.593 - 1)	52.1%
		Slope	0.706 (0.592 - 1)	0.078
	Beta	Pre-post	0.761 (0.658 - 1)	25.1%
		Slope	0.797 (0.686 - 1)	0.054
	Gamma	Pre-post	0.803 (0.671 - 1)	34.3%
		Slope	0.631 (0.529 - 1)	0.122
C4	Theta	Pre-post	0.729 (0.604 - 1)	49.5%
		Slope	0.655 (0.559 - 1)	0.138
	Alpha	Pre-post	0.747 (0.621 - 1)	46.9%
		Slope	0.710 (0.595 - 1)	0.104

	Beta	Pre-post	0.722 (0.605 - 1)	73.7%
		Slope	0.735 (0.606 - 1)	0.071
	Gamma	Pre-post	0.773 (0.634 - 1)	58.7%
		Slope	0.760 (0.634 - 1)	0.110
C3	Theta	Pre-post	0.878 (0.783 - 1)	49.8%
		Slope	0.771 (0.655 - 1)	0.010
	Alpha	Pre-post	0.682 (0.553 - 1)	47.7%
		Slope	0.619 (0.507 - 1)	0.078
	Beta	Pre-post	0.678 (0.565 - 1)	37.7%
		Slope	0.701 (0.583 - 1)	0.078
	Gamma	Pre-post	0.740 (0.618 - 1)	47.0%
		Slope	0.692 (0.567 - 1)	0.078

ICC, intraclass correlation coefficient; CI, confidence interval; SEM, standard error of measurement

Table 4. EMG variables test-retest ICC and SEM

EMG variable	Parameter	Test-retest ICC (95% CI)	Test-retest SEM
VL	Pre-post	0.722 (0.583 - 1)	29.5%
	Slope	0.623 (0.531 - 1)	0.083
RF	Pre-post	0.784 (0.686 - 1)	26.2%
	Slope	0.787 (0.675 - 1)	0.034
VM	Pre-post	0.767 (0.664 - 1)	25.5%
	Slope	0.728 (0.614 - 1)	0.044
BF	Pre-post	0.790 (0.680 - 1)	15.1%
	Slope	0.792 (0.685 - 1)	0.025
ST	Pre-post	0.727 (0.623 - 1)	11.4%
	Slope	0.656 (0.573 - 1)	0.020
CCI_{lat}	Pre-post	0.653 (0.551 - 1)	31.5%
	Slope	0.728 (0.583 - 1)	0.799
CCI_{med}	Pre-post	0.693 (0.576 - 1)	34.1%
	Slope	0.715 (0.596 - 1)	1.056

ICC, intraclass correlation coefficient; CI, confidence interval; SEM, standard error of measurement

Table 5. Corticomuscular coherence test-retest ICC and SEM

Coherence pair	Parameter	Test-retest ICC (95% CI)	Test-retest SEM
C3-VL	Pre-post	0.702 (0.577 - 1)	18.4%
	Slope	0.667 (0.551 - 1)	1365
C3-RF	Pre-post	0.728 (0.621 - 1)	23.4%
	Slope	0.775 (0.659 - 1)	1120
C3-VM	Pre-post	0.790 (0.683 - 1)	16.1%
	Slope	0.814 (0.714 - 1)	966
C3-BF	Pre-post	0.726 (0.626 - 1)	17.6%
	Slope	0.743 (0.633 - 1)	1140
C3-ST	Pre-post	0.771 (0.657 - 1)	12.6%
	Slope	0.781 (0.657 - 1)	787

ICC, intraclass correlation coefficient; CI, confidence interval; SEM, standard error of measurement

Brain and muscle activity during fatiguing maximum-speed knee movement

METHODS

Task

- Bilateral alternating 45-90° knee flexion
  - 8 x 10 s
  - 5 s rest
  - Maximum speed

Measurements

Corticomuscular coherence

Movement rate

EEG power (4 frontal and central electrodes)

EMG amplitude (knee flexors/ extensors)

OUTCOMES

(maximum-minimum within-task difference)

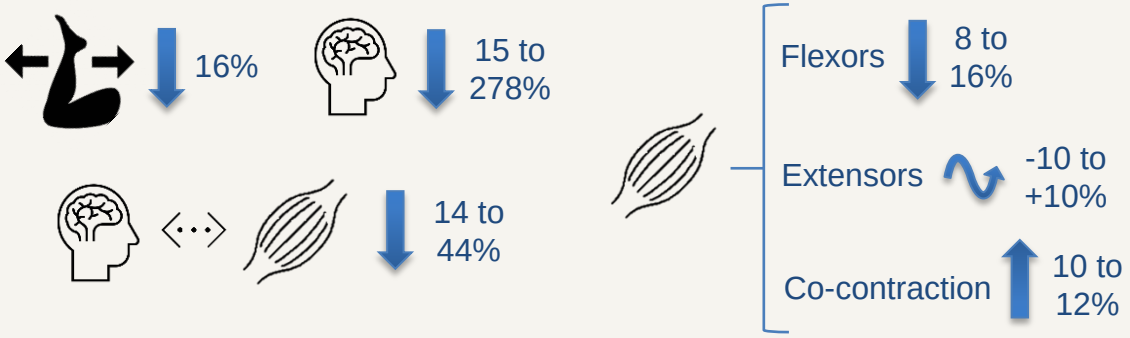

There was a significant decrease in knee movement rate, which was accompanied by a general decrease in EEG power (more notably at frontal electrodes), a decrease in normalized flexor EMG amplitude, an increase in flexor/extensor co-contraction, and a decrease in brain-muscle functional coupling.

CONCLUSION

Both central and peripheral changes were seen in association with knee motor slowing. However, no single measure seemed to determine task performance, suggesting that the interaction of changes at various levels was involved in performance regulation and fatigue.